Observation of multiple peaks in the magnetization curves of $NdBa_2Cu_3O_7$ single crystals

M. R. Koblischka, A. J. J. van Dalen,* T. Higuchi, K. Sawada, S. I. Yoo, and M. Murakami
Superconductivity Research Laboratory, International Superconductivity Technology Center, 1-16-25, Shibaura, Minato-ku, Tokyo 105, Japan
(Received 19 April 1996)

Induced current densities $j_s(T,B)$ were measured in a wide temperature ($5 \leqslant T \leqslant 90$ K) and field range ($0 \leqslant \mu_0 H_a \leqslant 7$ T) on single crystals of $NdBa_2Cu_3O_{7-\delta}$ using a superconducting quantum interference device magnetometer. The samples exhibit the fishtail or peak effect at temperatures above 30 K. In a small temperature window between 50 and 74 K, three peaks are seen in the $j_s(T,\mu_0 H_a)$ curves. The temperature and field behavior of the induced current densities is analyzed using a model describing a magnetization curve as composed of two independent contributions at low and high fields. By means of this analysis, it is demonstrated that the third peak corresponds to the fishtail peak, whereas the position of the second peak is practically independent of temperature. It is shown that the appearance of the second peak is due to the large values of the position of the fishtail peak. [S0163-1829(96)52334-9]

The fishtail or peak effect commonly found in magnetization curves of high-T_c superconductors as well as in conventional superconductors is widely discussed in the literature.[1–6] Recently, both in melt-processed and single-crystalline $NdBa_2Cu_3O_{7-\delta}$ samples, a fishtail peak twice as high as the central peak was found at $T=77$ K.[7] Moreover, due to the presence of the peak effect, the critical current density in the field range between 1 and 5 T is considerably enhanced, thus making $NdBa_2Cu_3O_{7-\delta}$ samples interesting candidates for applications. Therefore, it is strongly required to understand the mechanisms leading to the formation of the fishtail peak. Many approaches described the fishtail effect as being linked to a certain type of pinning center. However, only a general approach can explain all features of the fishtail effect reported in the literature, e.g., the dependence of the fishtail minimum on the sweep rate of the applied magnetic field[6] or the fishtail in heavy-ion irradiated samples.[8]

In Ref. 9, it was demonstrated that the shape of a magnetization loop is the result of an interplay between two pinning mechanisms with quite different field and temperature dependencies. One of them is active only at low fields, thus being responsible for the formation of the central peak in a magnetization curve and is vanishing rapidly with increasing field. The high-field mechanism is developing with increasing field, and its maximum causes under certain conditions the fishtail peak. Using this approach, magnetization curves with and without the fishtail shape can be modeled. If the central peak is wide enough (e.g., at low temperatures or in thin-film samples), the natural decrease of the high field component is effectively masked. However, when the central peak of the magnetization curve becomes sufficiently slender and/or small (typically at elevated temperatures above 40 K in the 123 system), the fishtail shape may be observed. A strong support for this scenario was found in the temperature scaling of the position (H_p) and height (j_p) of the fishtail peak measured on a $DyBa_2Cu_3O_{7-\delta}$ single crystal,[9] where a good scaling with the scaled field defined by $H_{sc}=H/(1-T/T^*)^p$ was obtained using the parameters $p=1.5$ and $T^* \approx T_c$. By means of this scaling, the high-field regime can be separated from the low-field contribution which was found to decay exponentially with raising field.

Within this framework, all features of the fishtail effect discussed in the literature can be explained. In the present paper, we performed such an analysis of induced current densities, $j_s(T,B)$, measured on a $NdBa_2Cu_3O_{7-\delta}$ single crystal which exhibits a magnetization curve with multiple pronounced peaks in a narrow temperature window.

The $NdBa_2Cu_3O_{7-\delta}$ single crystals are grown by a flux growth method in controlled oxygen atmosphere as described in Ref. 10. The crystal is twinned, and has the shape of a thin platelet with dimensions $0.79 \times 0.63 \times 0.08$ mm^3 with the c axis perpendicular to the sample surface. The sample shows a sharp transition to the superconducting state with a $T_{c,\mathrm{onset}}$ of 93.8 K. The homogeneity of the sample was tested by magneto-optical observations of the flux distributions using an iron-garnet indicator.[11] Magnetization loops are measured in the temperature range $5 \leqslant T \leqslant 90$ K using a Quantum Design MPMS-7 superconducting quantum interference device magnetometer equipped with a 7 T superconducting magnet. In order to avoid field inhomogeneities, the scan length is set to 15 mm. The magnetic field is applied parallel to the c axis of the sample. The induced current densities are calculated using the extended Bean model.

In Fig. 1, the induced current densities are shown as a function of the applied magnetic field in a semilogarithmic representation. In the temperature range $5 \leqslant T \leqslant 30$ K, the curves show the normal shape, i.e., the curves are monotonically decreasing with increasing applied field. After passing the central peak region (the position of the central peak will in the following be denoted by H_{p0}, and the corresponding current density by j_{p0}), j_s is practically independent of field in the measured field range. From 30 K on, a minimum in $j_s(\mu_0 H_a)$ can be detected indicating the onset of the fishtail behavior. However, the present sample shows another feature: At $T=50$ K and fields above 6 T, the $j_s(\mu_0 H_a)$ curves show a clear upwards curvature thus indicating the presence of another peak. A further increase of temperature causes then a fast decay of $j_s(\mu_0 H_a)$ as in a normal case. To clarify

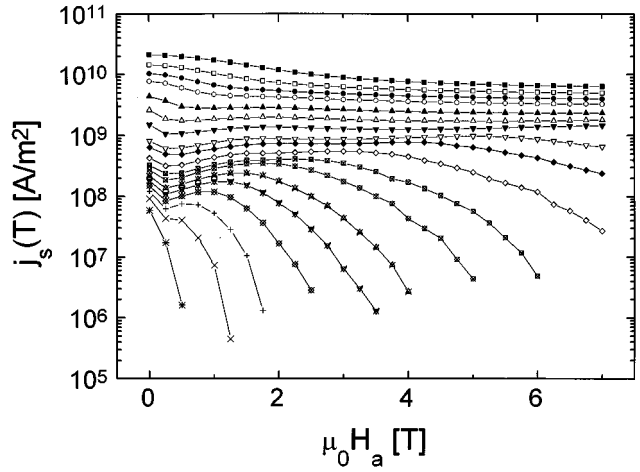

FIG. 1. Induced current densities, j_s, as function of the applied field $\mu_0 H_a$. The curves are measured at $T=$ 5, 10, 15, 20, 30, 40, 50, 60, 65, 70, 74, 77, 80, 82, 84, 86, 88, and 90 K (from top to bottom).

this situation, we followed the scaling approach described in Ref. 9. In a first attempt, the scaling was performed with the parameters $p=1.5$ and $T^*=T_c$. This scaling is relatively poor and works only at temperatures above 74 K. However, it gives clear evidence that indeed the third peak in the $j_s(\mu_0 H_a)$ curves is the *true* fishtail peak: The second peak at position H_{p1} is practically independent of temperature, whereas the third peak (position denoted by H_{p2}) scales as expected from the fishtail peak.[9]

To optimize the scaling, the $j_s(\mu_0 H_a)$ curves were added one after another to the scaled high-temperature curves. In this way, field scaling factors are obtained as a function of temperature as presented in the inset to Fig. 2. The line indicates the fit using $H_{sc}=H/(1-T/T^*)^p$ with T^* and p as

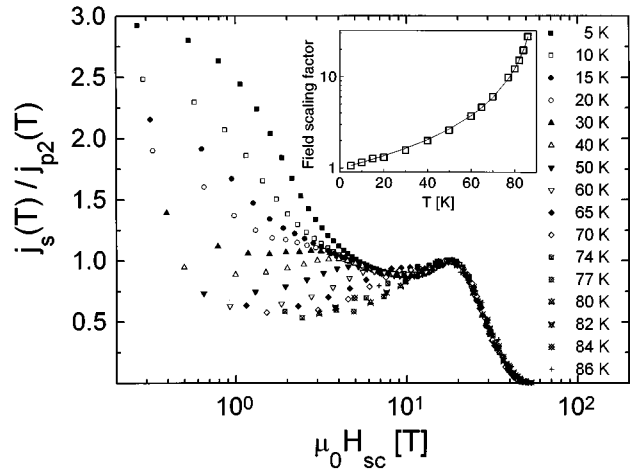

FIG. 2. The normalized induced current densities j_s/j_{p2} plotted versus the scaled field, $\mu_0 H_{sc}$. The temperatures are identical to fig. 1, except for the data at $T=88$ and 90 K. After scaling, the fishtail peak is found at a constant position $\mu_0 H_{sc}=18$ T. The scaling is working well at fields $H_a \geq H_{p2}$. For $H_a < H_{p2}$, the presence of the intermediate peak (30 K$\leq T\leq$ 74 K) and of the central peak (5 K $\leq T\leq$30 K) is disturbing the scaling. The inset presents the obtained field scaling factors as a function of temperature.

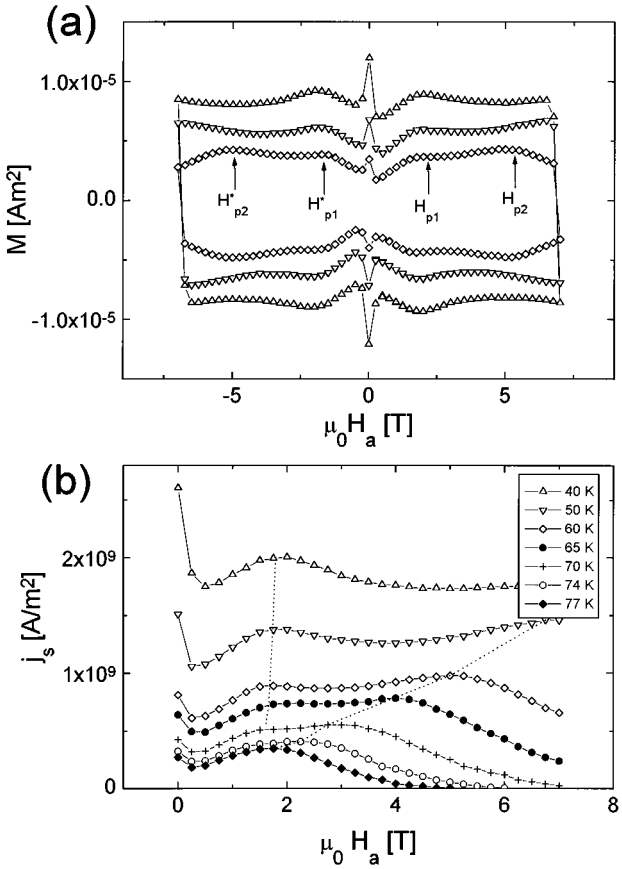

FIG. 3. (a): Magnetic moment, M, as a function of the applied field, H_a at $T=40$, 50 and 60 K, where the pronounced peaks can be observed. The measurement is performed counterclockwise. The peaks at H_{p1} and H_{p2} (H^*_{p1} and H^*_{p2} in negative fields) are present in all four quadrants of the magnetization curve. (b): Induced current densities at various temperatures as a function of the applied field.

fit parameters. The final result of the scaling is presented in Fig. 2, using $p=1.27$ and $T^*=92.9$ K. T^* is within the error margins equal to the independently determined $T_{c,\mathrm{onset}}$. The scaling of the $j_s(\mu_0 H_a)$ curves in the temperature range between 86 and 77 K is very good; starting from 77 K, a deviation at fields smaller than the scaled peak field can be found thus indicating the presence of the intermediate peak. Following Ref. 9, the scaling part of $j_s(\mu_0 H_a)$ corresponds to the pure high-field pinning mechanism, which is visible at the fishtail peak and at fields above H_{p2}. The data at low temperatures and low fields are affected by the central peak in the magnetization being caused by a different pinning mechanism. For the sample under study, also the presence of the intermediate peak causes a deviation from the general scaling.

In Fig. 3(a), full magnetization loops at $T=40$, 50, and 60 K are presented. Note that the peaks are present in all four quadrants of the magnetization curve, thus indicating that the pinning enhancement occurs independent of the direction of the field sweep. The peak positions $H_{p1,2}$ (decreasing field) and $H^*_{p1,2}$ (increasing field) are found to be identical. Figure 3(b) shows the current densities, j_s, as a function of the applied field in the temperature window 40 –77 K. At $T=$ 60 K, all three peaks and the corresponding minima can be

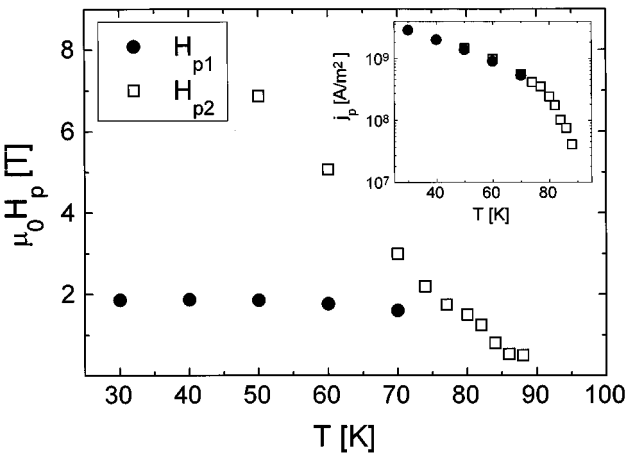

FIG. 4. The peak positions, H_{p1} and H_{p2}, as function of temperature. The position of the intermediate peak, $H_{p1}(T)$, is practically constant at 1.9 T, whereas the fishtail peak exhibits a large shift with temperature. The inset presents the corresponding peak currents, j_{p1} and j_{p2}, as function of temperature. Both peak currents depend exponentially on temperature up to 77 K.

resolved in the available field range. Above $T=74$ K, the two peaks merge together, and, as a result, the peak height of the remaining peak is found to increase as compared to other temperatures. It is important to point out that the first anomaly appearing in the magnetization curve at $T\approx 20$ K is the *intermediate* peak being visible as a shoulder to the central peak. Below 20 K, the broad central peak is dominant. The *fishtail* peak appears within the available field range only above $T=40$ K. In Fig. 4, the temperature dependence of the peak positions, H_{p1} and H_{p2}, is presented. $H_{p1}(T)$ is practically constant at $H_{p1}\approx 1.9$ T, in stark contrast to the behavior of $H_{p2}(T)$. The peak heights, j_{p1} and j_{p2}, however, are decaying in the same way exponentially with increasing temperature as presented in the inset to Fig. 4.

The measurements clearly confirm that the splitting of the $j_s(\mu_0 H_a)$ curves into a low-field and a high-field pinning regime also works in the case of $NdBa_2Cu_3O_{7-\delta}$ single crystals, showing the fishtail shape at different temperatures and fields than the $DyBa_2Cu_3O_{7-\delta}$ single crystals investigated in Refs. 6 and 9. However, this method does not discuss the origin of the enhanced pinning in the high-field range. Following Ref. 9, we may assume that all high-T_c materials have a high-field pinning mechanism which is very small at zero field and then raises until a maximum, j_p, is reached at the peak field, H_p, followed by a monotonous decrease of j_s at fields above H_p. It then depends on the sample geometry and on the critical current density at zero field, which influence the low-field behavior of the sample, whether a fishtail curve is obtained or not.[9]

For melt-processed $YBa_2Cu_3O_{7-\delta}$, Y_2BaCuO_5 (211) inclusions were proposed as a possible origin for the fishtail effect in Ref. 5. This is certainly not a general explanation for the fishtail effect itself. However, the peak size j_p, and its position, H_p, reflect the underlying microscopic pinning mechanism, so that differences between various samples can occur. For $NdBa_2Cu_3O_{7-\delta}$ single crystals, the position of the fishtail peak, H_{p2}, is typically at fields above 5 T at 60 K, thus enabling the observation of the intermediate peak at $H_{p1}<H_{p2}$.

For $NdBa_2Cu_3O_{7-\delta}$, a pinning mechanism was proposed,[7] which is due to a slight chemical variation of Nd and Ba atoms thus leading to regions with different T_c. The chemical composition of the Nd-123 system can, therefore, be written as $Nd(Ba_{1-x},Nd_x)_2Cu_3O_7$. With increasing external field, such regions may be driven normal, and can then contribute to pinning. The presence of such strong, additional pinning mechanisms can explain the large values found for both H_p and j_p.

The origin of the intermediate peak is a more complicated problem. It is important to point out that the visibility of this peak is strongly dependent on the position and shape of the other two peaks in the magnetization curve. If the central peak is very broad, the intermediate peak will be not visible at all or only in a very narrow temperature window. Additionally, also the width and the position of the fishtail peak are affecting the intermediate peak, which may degrade to a small shoulder or cause a very broad fishtail peak. This behavior explains why in typically large melt-processed $NdBa_2Cu_3O_{7-\delta}$ samples no three-peak magnetization curve is observed up to now. For most $YBa_2Cu_3O_{7-\delta}$ single crystals, the position of the fishtail peak is typically below 3 T in the whole temperature range, thus an additional peak in the magnetization curve would be completely suppressed.

A pinning mechanism independent of temperature is a matching or synchronization effect of the mean vortex lattice constant with the mean distance between microscopic pinning sites.[12] The largest pinning enhancement is achieved when the sample has a periodic arrangement of pinning centers. If the array is not perfect periodic, the peak will be a broad one due to statistical matching. If we calculate the mean vortex density via $a_0=2/\sqrt{3}\sqrt{\Phi_0/\mu_0 H_{p1}}$, we obtain $a_0=3.8\times 10^{-8}$ m, using $\mu_0 H_{p1}=1.9$ T. The resulting defect density would then be 6.9×10^{10} defects/cm^2. A clean proof of such a pinning mechanism could be given by the observation of higher harmonics,[12] which is, however, impossible due to the presence of the fishtail peak. Moreover, the position of the intermediate peak, H_{p1}, is found to vary between 1.9 and 3 T (i.e., a_0 is ranging between 38 and 30 nm, respectively) for various samples investigated.

Multiple peaks in magnetization curves are seen in other high-T_c superconductors as well. Andrä *et al.*[13] described multiple peaks in TlBaCaCuO-2223 and 2212 single crystals. As an explanation, the presence of various stacking sequences in the crystals was regarded, each characterized by a fishtail-shaped magnetization curve with its own characteristic H_p and j_p. However, such a mechanism would lead to various peaks in the magnetization curve, but each H_p should show a similar temperature dependence. Therefore, this cannot be the reason for the multiple peak magnetization loops described here.

Zhukov *et al.*[14] found a similar peak structure in an $YBa_2Cu_3O_{7-\delta}$ single crystal, which also showed very large H_{p2} values. $\mu_0 H_{p1}$ is ranging between 2 and 4 T, slightly shifting with increasing temperature. Oussena *et al.*[15] observed shoulders in the magnetization curve also at $\mu_0 H_{p1}\approx 2.5$ T. As a possible origin, pinning at twin boundaries was described. The values for H_{p1} found in Refs. 14 and 15 and our values would allow a matching at twin boundaries with a typical distance $d_0\approx 50$ nm.[16] A proof of such mechanism is complicated as detwinning requires an

oxygen treatment, which in turn can influence the shape of the central peak. The pinning effect of twins is still controversially discussed in the literature;[14,15,17] at low fields magneto-optical observations of flux patterns showed that twins (especially boundaries between different twin directions) act as channels for the vortices thus facilitating the flux movement. The values found for $H_{p1}(T)$ are all above the corresponding full penetration field, $H^*(T)$, so that the peak could be due to a vortex rearrangement as the geometrical flux pattern is heavily disturbed by the presence of twins.[11,18] These sample-geometry imposed effects are only observed in homogeneous, thin superconducting samples with H_a perpendicular to the surface, and not in bulk samples.

These observations clearly indicate that the appearance of such an intermediate peak may be a quite *common* feature of thin $R\mathrm{Ba}_2\mathrm{Cu}_3\mathrm{O}_7$ samples (R=rare earth), requiring only a large H_{p2} and a sufficiently slender central peak to be observed. Further measurements to identify the pinning centers responsible for the formation of the intermediate peak in $NdBa_2Cu_3O_{7-\delta}$, including the angular dependence of the induced currents, are in progress.

In conclusion, we have shown that in $NdBa_2Cu_3O_{7-\delta}$ single crystals $j_s(\mu_0 H_a)$ curves showing three pronounced peaks can be found. The scaling using $H_{sc}=H/(1-T/T^*)^p$ demonstrates clearly that the third peak in the $j_s(\mu_0 H_a)$ curves corresponds to the fishtail peak. The large value found for the position of the fishtail peak enables the observation of an intermediate peak in a narrow temperature window between 50 and 74 K. Experimental evidence is given that this peak may be caused by a matching effect at twin boundaries. Above $T=77$ K, the two peaks merge together and form one large single peak thus leading to high critical current densities.

This work was partially supported by New Energy and Industrial Technology Development Organization (NEDO) for the R & D of Industrial Science and Technology Frontier Program. M.K. and A.D. are grateful for support from Japanese Science and Technology Agency (STA).

*Present address: Materials Science Division, Argonne National Laboratory, Argonne, Illinois 60439.

[1] T. G. Berlincourt *et al.*, Phys. Rev. Lett. **6**, 671 (1961); J. Petermann, Z. Metallkunde **61**, 724 (1970).

[2] M. Däumling, J. M. Seuntjens, and D. C. Larbalestier, Nature **346**, 332 (1990); M. Osofsky *et al.*, Phys. Rev. B **45**, 4916 (1992).

[3] L. Krusin-Elbaum *et al.*, Phys. Rev. Lett. **69**, 2280 (1992).

[4] K. A. Delin *et al.*, Phys. Rev. B **46**, 11 092 (1992); L. F. Cohen *et al.*, Cryogenics **33**, 352 (1993); Y. Yeshurun *et al.*, Phys. Rev. B **49**, 1548 (1994); M. Werner *et al.*, Physica C **235-240**, 2833 (1994).

[5] M. Ullrich *et al.*, Appl. Phys. Lett. **63**, 406 (1993).

[6] A. J. J. van Dalen *et al.*, Physica C **250**, 256 (1995).

[7] M. Murakami *et al.*, Jpn. J. Appl. Phys. **33**, L715 (1994); S. I. Yoo *et al.*, Appl. Phys. Lett. **65**, 633 (1994).

[8] M. R. Koblischka *et al.*, Physica C **235-240**, 2839 (1994).

[9] M. Jirsa *et al.* (unpublished).

[10] K. Sawada *et al.* (unpublished).

[11] M. R. Koblischka and R. J. Wijngaarden, Supercond. Sci. Technol. **8**, 199 (1995).

[12] A. M. Campbell and J. E. Evetts, *Critical Currents in Superconductors* (Taylor & Francis, London, 1972), p. 194, and references therein.

[13] W. Andrä *et al.*, Physica C **213**, 471 (1993).

[14] A. A. Zhukov *et al.*, Phys. Rev. B **51**, 12 704 (1995).

[15] M. Oussena *et al.*, Phys. Rev. B **51**, 1389 (1995).

[16] M. Rand *et al.*, Cryogenics **33**, 291 (1993).

[17] V. K. Vlasko-Vlasov *et al.*, Phys. Rev. Lett. **72**, 3246 (1993).

[18] Th. Schuster *et al.*, Phys. Rev. B **49**, 3443 (1994).